

# Performance Analysis and Working Fluids Selection of Organic Rankine Cycle in a Triple Power Generation System Combined with Gas Turbine and Solid Oxide Fuel Cell Cycles

Jamasb Pirkandi<sup>1,\*</sup>, Arman Maroufi<sup>2</sup>, Hossein Penhani<sup>1</sup>

<sup>1</sup> Faculty of Aerospace, Malek Ashtar University of Technology, Iran

<sup>2</sup> Faculty of Industrial and Mechanical Engineering, Islamic Azad University, Qazvin Branch, Qazvin, Iran

## Article Information

Article History:

Received:

05 Sep 2022

Received in revised form:

29 Nov 2022

Accepted:

05 Jan 2023

## Keywords

organic Rankine cycle

Solid oxide fuel cell

Gas turbine

Exergy

Combined cycle

## Abstract

The main target of this research is to model, analyze, and compare the performance of two hybrid systems, 1. A gas turbine (GT) and steam Turbine (ST) plus a solid oxide fuel cell (SOFC) and 2. a hybrid GT, ORC, and SOFC cycle (SOFC+ GT+ ORC) from the thermodynamic and exergy perspectives. Studies show that the output power of a combined system with a steam cycle is higher than that of a system with an organic Rankine cycle, but this higher output does not necessarily mean that this cycle performs better. Therefore, a steam cycle at a higher power range and turbine inlet gas temperature is more justified. The results show that among the analyzed fluids, the use of toluene fluid in the organic Rankine cycle produces the most power at a condenser temperature of 319 Kelvin.

## 1. Introduction

The worldwide excessive and careless utilization of fossil fuels and the extensive pollution caused by

burning such fuels has prompted many researchers to try and develop novel and highly efficient energy conversion techniques and systems. Additionally, the global energy crisis has also compelled scientists and

\*Corresponding Author: : jpirkandi@mut.ac.ir

engineers to take practical steps to improve and optimize energy-producing and energy-consuming equipment and appliances. Gas and steam turbines, reliable energy-producing equipment with varied applications, have long been used in various industries, and numerous researchers have attempted to optimize the performance of these devices [1-5]. For example, older turbine optimization methods are costly, ineffective, and incapable of substantially boosting the output power of these two cycles. In a relatively new approach, gas turbine (GT) and steam turbine (St) cycles have been combined to form a combined system whose net power output and efficiency are greater than those of each cycle alone [6-8]. With the development of fuel cells in recent years, many researchers have considered combining them with other energy systems. Among fuel cell types, solid oxide fuel cells (SOFCs) have exhibited good potential for hybridization with other systems in power plant cycles due to their high operating temperature. Many researchers have eagerly investigated the combination of solid oxide fuel cells with a gas turbine cycle in recent years [9-14]. Moreover, it is possible to recover the existent heat from such systems due to the high-temperature exhaust gases from these hybrid cycles. The main purpose of this research is to use a highly efficient steam cycle in the downstream of a gas turbine-fuel cell hybrid cycle in order to form a triple hybrid system.

Lai et al. [14] comprehensively reviewed macroscopic SOFC and SOFC/GT hybrid system models. The energy, economic, exergy, and environmental analysis of three different GT-SOFC systems were performed by Eisavi et al. [15]. Huang and Turan built a novel model with thermodynamic processes to gain operational and energetic insights into the SOFC/GT hybrid system [16]. They show that by a recuperator effectiveness of 0.9, 68% electric efficiency can be achieved. Hedberg et al. introduced a fuel cell-GT hybrid cycle with high thermal efficiency from a topping/bottoming cycle without a high-temperature heat exchanger [17].

Guo et al. proposed a novel SOFC-GT based system, which integrated a TRCC with a LNG cold energy utilization system [18]. Azizi and Brouwer presented the design, analysis, and optimization of (SOFC/GT) hybrid systems for different system configurations [19]. The thermodynamic analysis of an integrated system consisting of a steam-gas turbine and SOFC was studied by Pirkandi et al. [20]. Ezzat and Dincer investigated a new combined power plant with two main powering sources, a GT cycle and ammonia fed SOFC [21]. Modeling and optimization of a new integrated system consisting of a SOFC, a gas turbine, and a supercritical carbon dioxide Brayton cycle have been done by Chen et al. [22]. Al-Hamed and Dincer investigated a new ammonia and SOFC system for clean electric rail transportation [23]. Three different configurations fed by biomass and based on advanced technologies have been considered and analyzed by Minutillo et al. [24]. Yuksel et al. thermodynamically studied a biomass-based integrated power plant [25]. Gholamian and Zare investigated Kalina and Organic Rankine cycles for waste heat recovery from a combined SOFC-GT system [26]. Kim et al. introduced a novel 5-kW class of SOFC based combined power generation system [27], and Sadat et al. examined a novel plant driven by a SOFC unit [28]. Mehrpooya et al. [29] investigated the biodiesel and glycerol processes, SOFC, and ORC for the production of electricity and biodiesel simultaneously.

A survey of the literature indicates that most researchers have paid less attention to triple hybrid systems, with most articles focusing on dual integrated systems such as gas turbines and fuel cells or gas turbines and steam cycles. In this study, first, a triple-integrated system of a gas-steam cycle and fuel cell (GT+St+SOFC) was analyzed from thermodynamics and exergy standpoints. Then, the following section considered a steam cycle instead of an organic Rankine cycle, and its performance was investigated. And finally, in the last section, the results of the triple combined sys-

tem with an organic Rankin cycle were compared with the previous section.

## 2. Introducing the proposed system

The main target of this research is to use a high-efficiency cycle in the downstream of the GT-SOFC to form a triple combined system. The constituent components of this triple system have been introduced below.

### 2.1. Steam cycle

Considering the importance of the steam cycle in the proposed system, we tried to use an appropriate high-efficiency steam cycle in this research. For this purpose, nine different configurations of this cycle were examined, and ultimately, the best arrangement was chosen for this purpose. The schematic of this proposed steam cycle are displayed in Fig. (1), and the full results of this research have been presented in the Pirkandi et al. study [20].

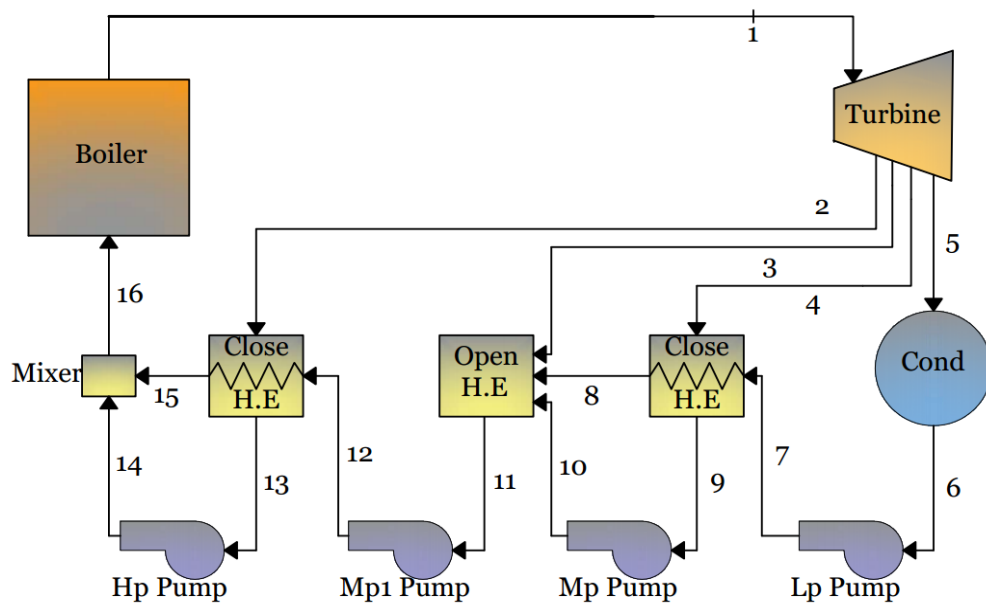


Fig. 1. Configuration of the Rankin cycle with one open and two closed regenerators [20].

### 2.2. Hybrid cycle of GT+SOFC

SOFC can be satisfactorily combined with GT cycles because of their high operating temperature. This combination could be direct (using a common working fluid) or indirect (using a non-common working fluid). In direct hybridization, a GT cycle can be combined with a pressurized fuel cell or under

atmospheric ambient conditions. Investigations show that direct pressurized hybrid cycles performance is better than other integrated systems. Therefore, considering the above, a directly-connected and pressurized integrated cycle of GT and SOFC will be used in this research. A schematic of this hybrid system is illustrated in Fig. 2.

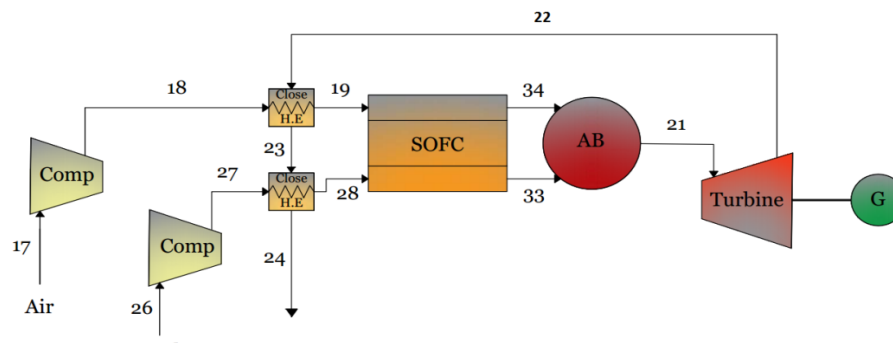


Fig. 2 Schematic of the GT+SOFC hybrid system.

### 2.3. Combined GT, SOFC, and steam cycle

A triple combined system was obtained using the best arrangement mentioned in [20]. A schematic of this hybrid system is illustrated in Fig. 3. This system includes a SOFC stack with internal reforming, an afterburner chamber, GT, air and fuel compressors, air and fuel regenerators, a steam generator (boiler), four water pumps, condenser, open heat regenerator and two closed heat regenerators for steam, and a steam turbine. The fuel utilized in the system was natural gas with a composition of 97%  $\text{CH}_4$ , 1.5%  $\text{CO}_2$ , and 1.5%  $\text{N}$ , and the air was composed of 21%  $\text{O}_2$  and 79%  $\text{N}_2$ . First, the air and the natural gas entering the cycle are compressed by compressors and heated before entering the fuel cell. The reaction of hydrogen, produced by natural gas, with oxygen in the fuel cell produces a considerable amount of electrical power, producing the efficiency increment of the combined system. Down the line, the fuel cell outlet gases that did not participate in reforming reactions enter the afterburner chamber and react with each other. Then, the output from the production chamber enters the GT and produces work. Finally, the hot exhaust gases from the turbine enter into three heat regenerators. The first two regenerators are used for preheating the air-fuel mixture that comes into the fuel cell, and the

third regenerator is employed to produce hot steam for the Rankin cycle. In the steam cycle, first, the superheated steam produced in the heat regenerator of the boiler enters the turbine. Then, the outlet flow from the steam turbine then enters the condenser and loses its heat there. Three branches are taken from the turbine to preheat the outlet condenser flow. Next, the water leaving the condenser is passed through a closed low-pressure heat exchanger and pumped to the open heat exchanger, where the outlet water combines with the outlet flows of branches 3 and 4. After passing the closed high-pressure heat exchanger, all these flows are finally combined with the outlet flow of branch 2 and returned to the heat regenerator of the boiler to complete the cycle.

In the analysis of the proposed triple hybrid system, the following assumptions are considered:

- All the components of the cycle are assumed adiabatic.
- Fluid flow is steady in all components.
- Changes in potential and kinetic energy are negligible.
- The ideal behavior of gas is assumed.
- The leakage of gas inside the system to the outside

is ignored.

- The pressure and temperature of gases coming out of the anode and cathode are assumed to be the same and equal to the battery's temperature and working pressure.
- The chemical components and temperature and pressure distribution inside the fuel cell have been neglected.
- The voltage under the fuel cell stacks is assumed to be constant.
- The steam generator's heat exchanger is assumed to be a simple exchanger, and the details of its modeling, such as determining the pinch temperature, have been omitted.
- The temperature of air and fuel entering the system is assumed to be the same.
- The operating fluid at the outlet of the condenser and the inlet of the pump is a saturated liquid.
- For the pump and turbine, isentropic efficiency is considered as input.

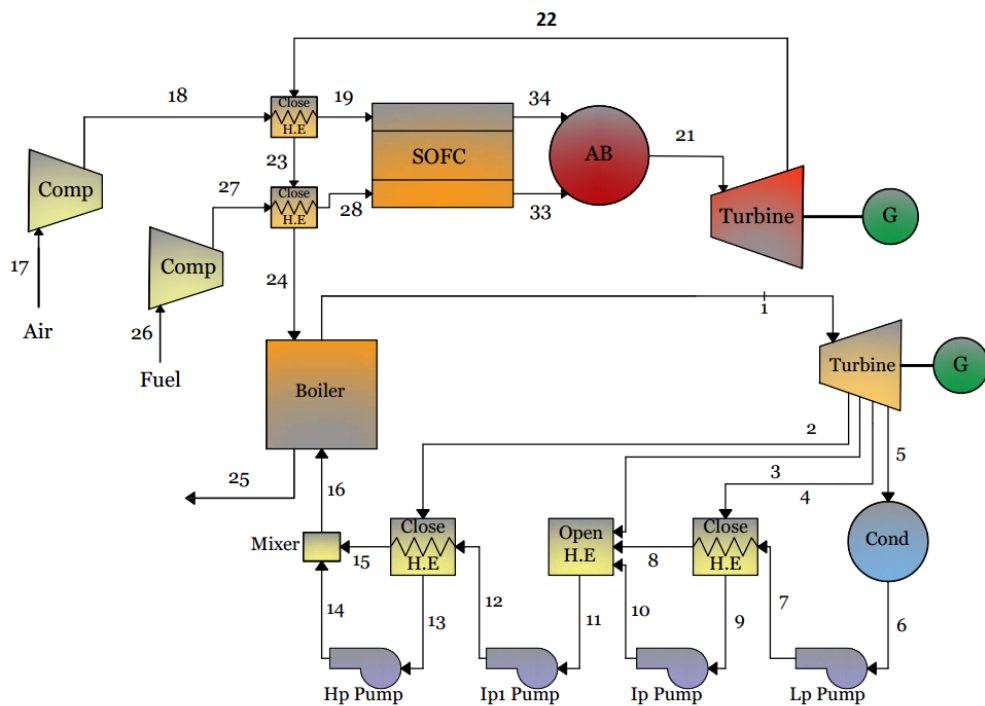


Fig. 3 The schematic of the GT+SOFC+St combined system.

### 3. Governing equations

The governing equations of each component of the

proposed cycle are presented in the Table 1. Additional relationships are available in Reference [20].

**Table 1. governing equations of each component of the proposed cycle [20].**

Component	equations	Number
<b>Compressor</b>	$\frac{T_{18s}}{T_{17}} = \left( \frac{P_{18}}{P_{17}} \right)^{\frac{\kappa_c - 1}{\kappa_c}}$	(1)
	$\eta_{ca} = \frac{W_{c,s}}{W_c} = \frac{\bar{h}_{18s} - \bar{h}_{17}}{\bar{h}_{18} - \bar{h}_{17}} = \frac{T_{18s} - T_{17}}{T_{18} - T_{17}}$	(2)
	$\dot{W}_{ca} = \dot{n}_a \times (\bar{h}_{18} - \bar{h}_{17})$	(3)
<b>Fuel cell</b>	$E = E^o + \frac{R_c \times T}{n_c \times F} \ln \left( \frac{P_{H_2} \times P_{O_2}^{0.5}}{P_{H_2O}} \right)$	(4)
	$V_{cell} = E - (V_{act} + V_{ohm} + V_{conc}) = E - \Delta V_{loss}$	(5)
	$I_{cell} = \dot{i} \times A_{cell}$	(6)
	$(\dot{W}_{DC})_{sofc} = V_{cell} \times I_{tot}$	(7)
	$(\dot{W}_{AC})_{sofc} = (\dot{W}_{DC})_{sofc} \times \eta_{m,SOFC}$	(8)
	$I_{tot} = n \times I_{cell} = 2Fz$	(9)
	$\dot{Q}_r = x(\bar{h}_{CO} + 3\bar{h}_{H_2} - \bar{h}_{CH_4} - \bar{h}_{H_2O})$	(10)
	$\dot{Q}_{sh} = y(\bar{h}_{CO_2} + \bar{h}_{H_2} - \bar{h}_{CO} - \bar{h}_{H_2O})$	(11)
	$\dot{Q}_{elec} = zT\Delta S - I\Delta V_{Loss}$	
	$\Delta S = \left( S_{H_2O} - S_{H_2} - \frac{1}{2}S_{O_2} \right) + \frac{R_u}{2} \ln \left( \frac{P_{H_2}^2 \times P_{O_2}}{P_{H_2O}^2} \right)$	(12)
	$\dot{Q}_{net} = \dot{Q}_{sh} + \dot{Q}_{elec} - \dot{Q}_r$	(13)
	$\sum \dot{n}_{in} h_{in} = \dot{Q}_{sur} + \dot{W}_{SOFC} + \sum \dot{n}_{out} h_{out}$	(14)
	<b>Afterburner chamber</b>	$\sum \dot{n}_{in} h_{in} - \sum \dot{n}_{out} h_{out} - \dot{Q}_{loss,ab} = 0$
$\dot{Q}_{loss,ab} = \dot{n}_{fuel} \times (1 - U_f) \times (1 - \eta_{ab}) \times LHV$		(16)
<b>Gas turbine</b>	$\frac{T_{21s}}{T_{22}} = \left( \frac{P_{21}}{P_{22}} \right)^{\frac{\kappa_g - 1}{\kappa_g}}$	(17)
	$\eta_{GT} = \frac{W_{GT,s}}{W_{GT}} = \frac{\bar{h}_{21} - \bar{h}_{22}}{\bar{h}_{21} - \bar{h}_{22s}} = \frac{T_{21} - T_{22}}{T_{21} - T_{22s}}$	(18)
	$\dot{W}_{GT} = \dot{n}_{21} \times (\bar{h}_{21} - \bar{h}_{22})$	(19)
<b>Air and fuel heat regenerators</b>	$\mathcal{E} = \frac{T_{19} - T_{18}}{T_{22} - T_{18}}$	(20)
	$\dot{n}_{18} \times (\bar{h}_{19} - \bar{h}_{18}) = \dot{n}_{22} \times (\bar{h}_{22} - \bar{h}_{23})$	(21)
<b>Turbine</b>	$\eta_T = \frac{W_{T,s}}{W_T} = \frac{\bar{h}_{in} - \bar{h}_{out}}{\bar{h}_{in} - \bar{h}_{out,s}}$	(22)
	$\dot{W}_T = \dot{m}_1 h_1 - \dot{m}_2 h_2 - \dot{m}_3 h_3 - \dot{m}_4 h_4 - \dot{m}_5 h_5$	(23)
<b>Condenser</b>	$\dot{m}_5 h_5 = \dot{Q}_{out} + \dot{m}_6 h_6$	(24)
	$\dot{m}_5 = \dot{m}_6$	(25)
<b>Pump</b>	$\dot{W}_{p,s} = \dot{m}_6 (P_7 - P_6)$	(26)
	$\eta_{\lambda,pump} = \frac{W_{p,s}}{W_p}$	(27)
<b>Mixing chamber</b>	$\dot{m}_{15} h_{15} + \dot{m}_{14} h_{14} = \dot{m}_{16} h_{16}$	(28)
	$\dot{m}_{15} + \dot{m}_{14} = \dot{m}_{16}$	(29)
<b>Hybrid system</b>	$\eta_{elec} = \frac{W_{net}}{\dot{n}_{fuel} \times LHV}$	(30)
	$\dot{W}_{net} = \dot{W}_{sofc} + \dot{W}_{GT} + \dot{W}_T - \sum \dot{W}_p - \sum \dot{W}_c$	(31)
<b>Exergy</b>	$\sum (1 - \frac{T_o}{T}) \dot{Q}_k + \sum \dot{E}_i = \sum \Psi_w + \sum \dot{E}_o + \dot{i}_{destroyd}$	(32)
	$\dot{E}^{\dot{}} = \dot{E}^{\dot{}}_{ph} + \dot{E}^{\dot{}}_{ch}$	(33)
	$\dot{E}^{\dot{}}_{ph} = \dot{m}[(h - h_o) - T_o(s - s_o)]$	(34)
	$\dot{E}^{\dot{}}_{ch} = \dot{m}[\sum_i y_i \bar{e}_{ch,i} + R_u T_o \sum_i y_i \ln y_i]$	(35)

## 4. Solution method

This research investigates the parameters that influence the functioning of the steam cycle, including the pressure and temperature of the steam generator, condenser pressure, and the different working fluids used in the steam cycle (organic Rankin cycle). A computer code has been written in EES software for modeling the proposed hybrid system. In the first part of this computer code, the nonlinear electrochemical and reforming equations are simultaneously solved with the thermal equations of the fuel cell. The results include output chemical products, current, voltage, temperature, voltage loss, efficiency, generated power, etc. Contrary to most former studies, the fuel cell's working temperature was not assumed constant in this study and was calculated for different working conditions. In the second part of the computer program, the entire hybrid cycle was investigated, and the results were reported.

## 5. Results

Here, the performances of the proposed cycle, the triple integrated system with the steam or organic

Rankin cycle, have been evaluated. The parameters examined in these analyses are condenser pressure, boiler temperature and pressure, and the working fluid used in the organic Rankin cycle.

### 5.1. Validation

In order to check the validation of the present computer code, the results of this research were compared with those obtained from several credible references. Considering the novelty of the research topic and a lack of sufficient data in this field, this comparison has been made separately for different sections of the examined hybrid system. First, a computer code was written for the fuel cell and gas turbine [GT+SOFC], and then the results were validated. Then, another program was written for the Rankin steam cycle and the organic Rankin cycle, and the obtained results were compared. Finally, after validating the results of both systems, the two cycles were integrated.

#### 5.1.1. Validating the GT-SOFC hybrid cycle

In order to validate the proposed code written for the GT-SOFC hybrid cycle, the cycle introduced by Chan et al. [30] was first investigated, and then the two were compared, as illustrated in Table 2. A computational error of 1.2% between the two cycles confirms the validity of the written code.

**Table 2.** Comparison of present research results with Chen et al. [30].

Error %	present research	Chan et al. [30]	Parameters
0.49	61.89	62.2	Electrical efficiency of the system
1.2	0.7289	0.738	Cell voltage (v)
0	1416	1416	Current density (A/m <sup>2</sup> )
0	1166	1166	Cell operating temperature (K)

### 5.1.2. Validating the proposed steam cycle

The cycle presented by Cengel [31] was modeled to validate the section related to the steam cycle. This model includes a simple steam cycle with known val-

ues of inlet and outlet temperatures. According to Table 3, a computational error of 0.1% exists between the results under equal conditions, which shows the validity of the computer code written by considering the cycle presented in [31].

**Table 3. Comparison of the present research results with those obtained by Cengel [31].**

Error %	present research	Cengel et al. [31]	Parameters
0.077	26.02	26	Electrical efficiency of the system
0.06	709.5	709.07	Output power of the system (kJ / kg)
0.032	2727	2727.88	Inlet heat to the system (kJ / kg)
0.09	2017	2018.81	Exit heat from the system (kJ / kg)
0.045	0.8856	0.886	Steam quality (x)

### 5.1.3. Validating the organic Rankin cycle

In this section, the organic Rankin cycle was validated. For this purpose, the Song et al. [32] cycle has been analyzed. The results of the present research and [32], obtained under equal input

conditions and with the consideration of working fluid R123, have been compared in Table 3. As is observed, a computational error of 7.93% exists between the present results and the results in reference [32], which confirms the validity of the code for this section.

**Table 4. Comparison of the present research results with those obtained by Song et al. [32].**

Error %	Song et al. [32]	present research	Parameters
0	393.7	393.7	Steam generator temperature (K)
0	1211	1211	Steam generator pressure (kPa)
2.67	13.5	13.14	Electrical efficiency of the system
7.93	534	580	Output power of the system (kW)

## 5.2. Analyzing the results of the steam cycle

In this section, a parametric analysis of the steam cycle was performed with regard to the decision variables of condenser pressure and the temperature and pressure of the steam generator (boiler). Fig. 4 indicates the electrical efficiency of the steam cycle versus condenser pressure and boiler temperature. As is observed, the cycle's electrical efficiency diminishes with the surge of condenser pressure and increases with the increment of boiler temperature. The increase in condenser pressure causes the steam cycle to dissi-

pate heat to the environment at a higher temperature. Considering the philosophy of steam cycle design, which is based on heat dissipation at the least possible temperature (definition of Carnot efficiency), the abovementioned phenomenon reduces the power generation potential of the cycle and, consequently, lowers its electrical efficiency. The rise of boiler temperature actually means heat absorption at higher temperatures; which, according to the definition of Carnot efficiency, leads to the increase of the steam cycle's electrical efficiency.

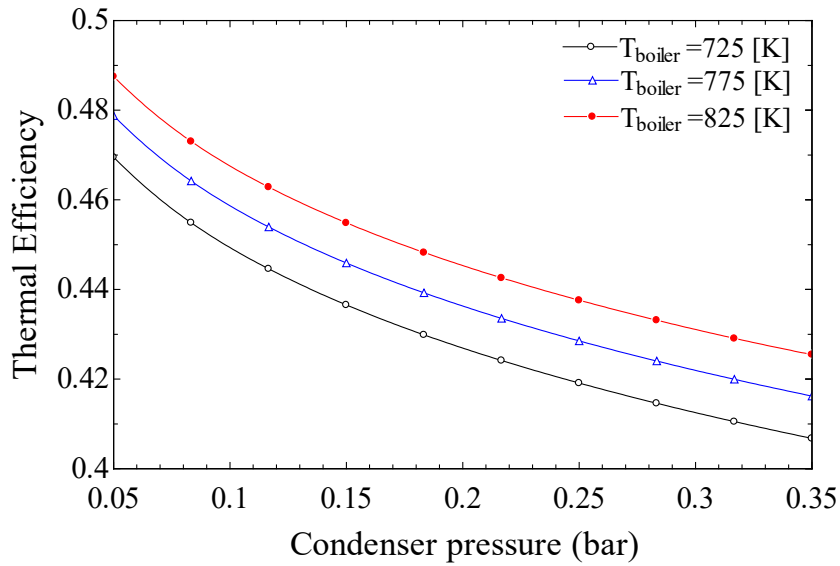


Fig. 4. Electrical efficiency of the steam cycle versus condenser pressure for different boiler temperatures.

Fig. 5 illustrates the exergy efficiency of the steam cycle versus condenser pressure and boiler temperature. According to this figure, the exergy efficiency of the cycle diminishes with the rise of condenser pressure. Considering the reduction of output power due to the increase in condenser pressure, these changes seem to

be reasonable. The results also indicate that exergy efficiency diminishes with the rise of steam generator temperature. The reasons for the decrease in exergy efficiency in this cycle are the higher utilization of fuel and the increase of irreversibility rates in cycle components, especially in the boiler.

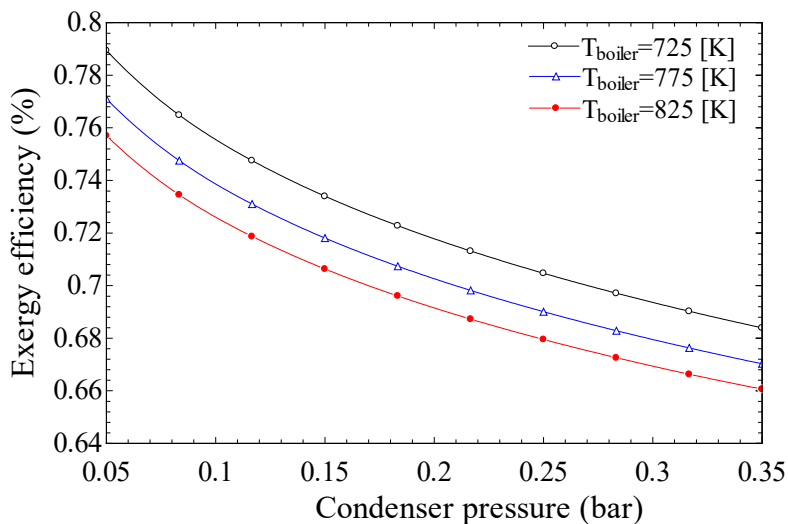


Fig. 5. Exergy efficiency of the steam cycle versus condenser pressure for different boiler temperatures.

Fig. 6 displays the power output of the steam cycle versus condenser pressure and boiler temperature. As mentioned before, the surge of condenser pressure leads to the rise of temperature during heat dissipation

in the cycle, and this causes the cycle's output power to diminish. The increase of boiler temperature due to the temperature rise during heat absorption leads to the surge of output power from the steam cycle.

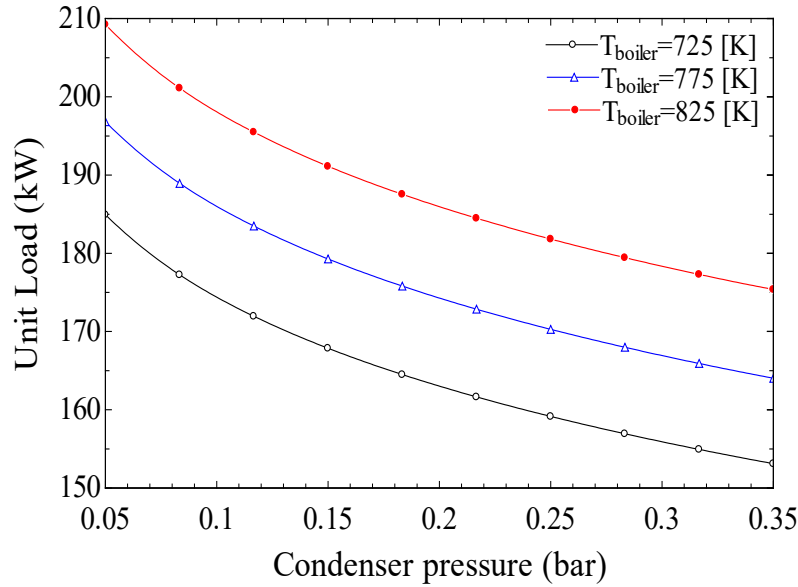


Fig. 6. Power output of the steam cycle versus condenser pressure for different boiler temperatures.

Fig. 7 shows the exergy destruction rate of the steam cycle versus condenser pressure and also the boiler temperature. The obtained results indicate that with the rise of boiler temperature, the rate of exergy destruction (one cause of irreversibility in the cycle) increases. Among the cycle components, the boiler has the highest exergy destruction rate, which seems to

be justified, considering the high fuel consumption and the increase of entropy generation in the cycle. By varying the condenser pressure, no significant change is observed in the exergy destruction rate. Findings reveal that the rise of boiler temperature has a greater influence on the exergy destruction rate than the increase of condenser pressure.

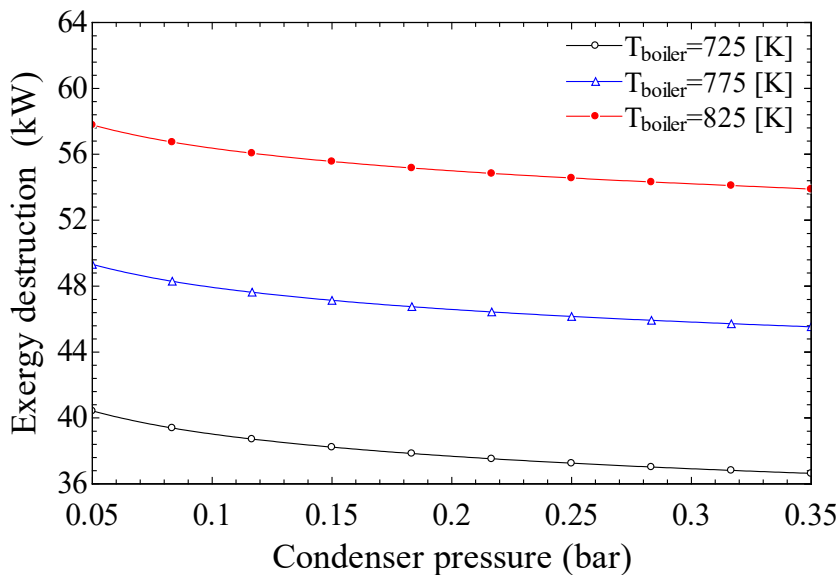


Fig. 7. Exergy destruction rate of the steam cycle versus condenser pressure for different boiler temperatures.

Fig. 8 illustrates the steam cycle's exergy loss rate versus condenser pressure and boiler temperature. According to this figure, the rate of exergy loss (another cause of irreversibility in the cycle) rises with the increment of boiler temperature as well as increasing the condenser pressure. As is observed, the increase in condenser pressure has a considerably greater ef-

fect on the rate of exergy loss than the rise in boiler temperature. Considering the dissipation of a large amount of energy in the condenser and the fact that the condenser has the highest exergy loss among the cycle components, the whole cycle will be affected by changing the operating conditions (working temperature and pressure) of the condenser.

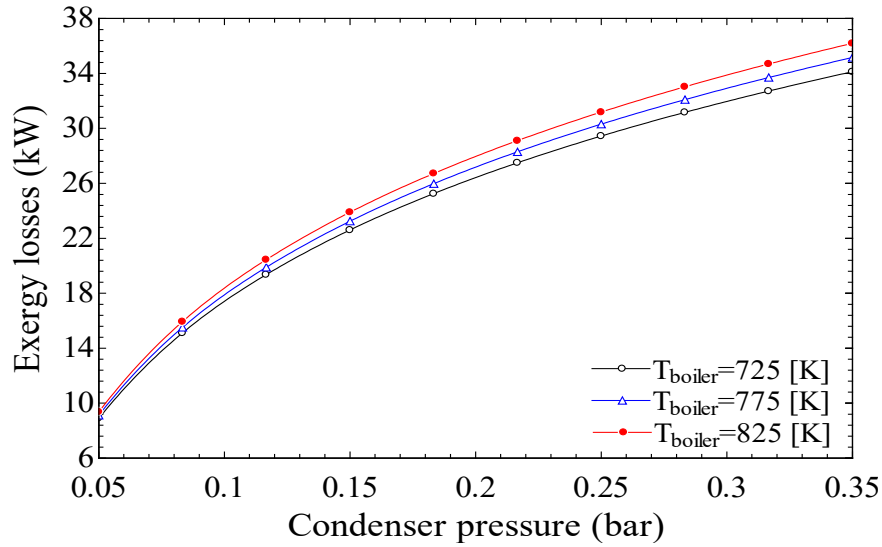


Fig. 8. Rate of exergy loss in the steam cycle versus condenser pressure for different boiler temperatures.

The effect of boiler pressure on the efficiency of the steam cycle is evaluated below. Fig. 9 shows the electrical efficiency of the steam cycle versus boiler temperature and pressure. As is observed, the system's electrical efficiency increases with the boiler tempera-

ture and pressure. This is because boiler pressure determines the lowest possible temperature needed for heat absorption, and this minimum temperature for the boiler increases with the rise of boiler pressure, thereby boosting the electrical efficiency of the system.

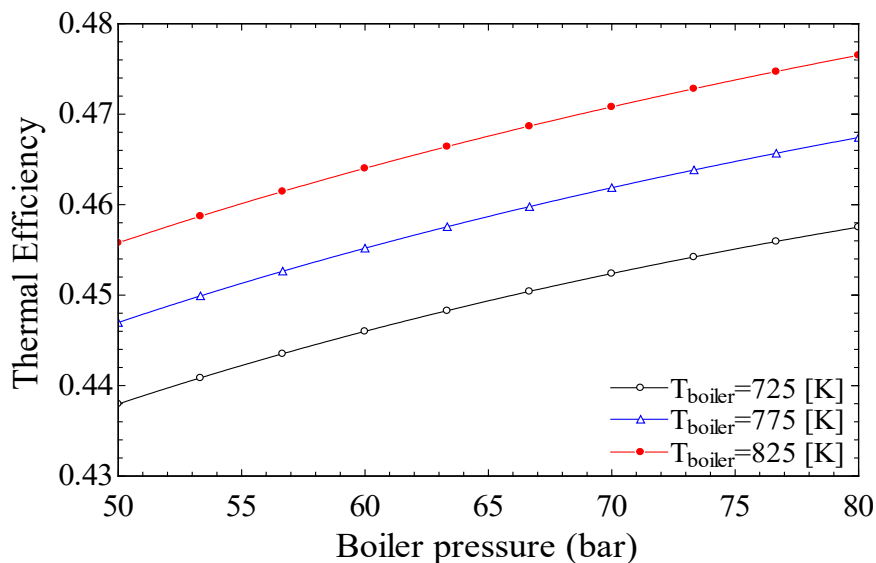


Fig. 9 Electrical efficiency of the steam cycle versus boiler pressure for different boiler temperatures.

The variations of exergy efficiency versus boiler temperature and pressure have been plotted in Fig. 10. The obtained results show that the rise of boiler pressure leads to the surge of output power and, thus, the

increase of exergy efficiency. Exergy efficiency diminishes with the rise of boiler temperature. This is caused by the increased rate of irreversibility in the system due to the escalation of fuel consumption.

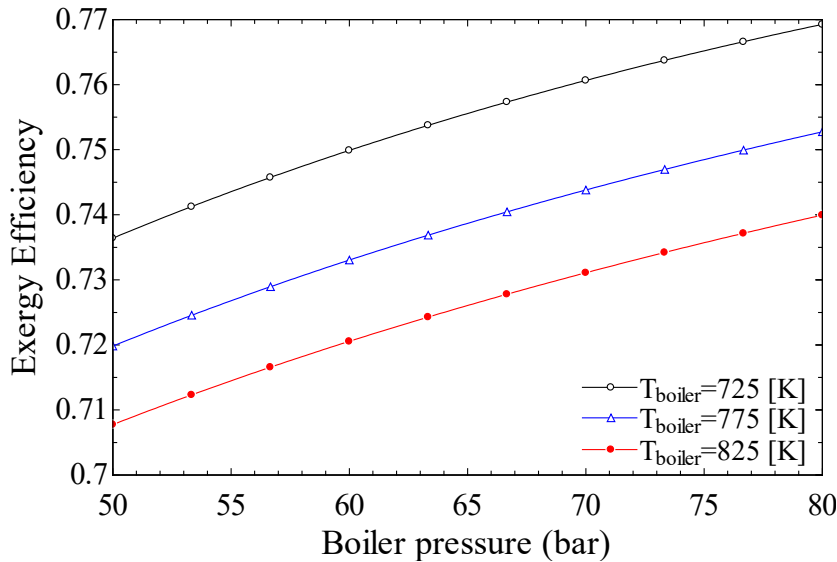


Fig. 10. Exergy efficiency of the steam cycle versus boiler pressure for different boiler temperatures.

Fig. 11 illustrates the output power of the steam cycle versus boiler pressure and temperature. According to this figure, the output power of the cycle goes up as the boiler pressure and temperature rise. The results show that the increase in output power is influenced more by boiler temperature than boiler pressure. Boiler pres-

sure is proportional to steam saturation temperature during the steam absorption process, while, by superheating the steam, the boiler temperature will always be greater than the saturation temperature. The considered temperature for computing the Carnot efficiency of the steam generating cycle is the temperature of superheated steam.

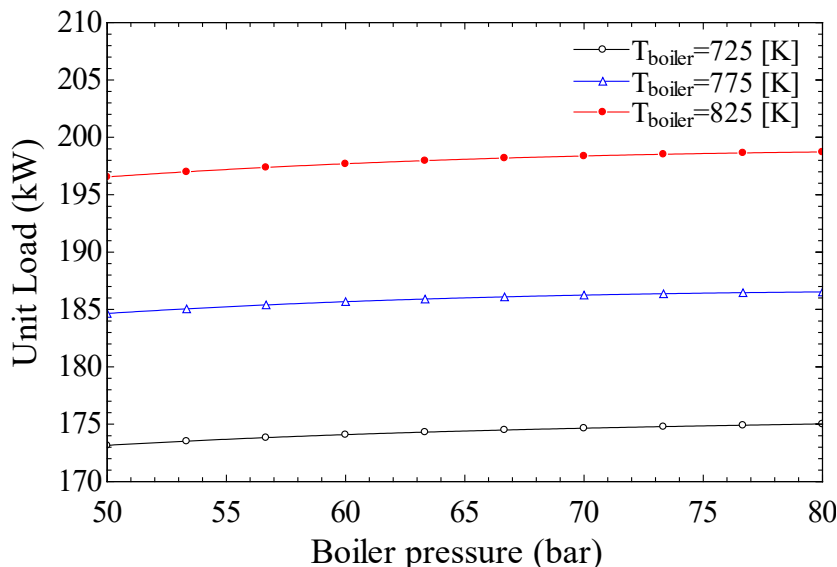


Fig. 11. Power output of the steam cycle versus boiler pressure for different boiler temperatures.

Figures 12 and 13 show the exergy destruction rate and exergy loss in the steam cycle versus boiler pressure and temperature, respectively. As expected, based on the above results, the rise of boiler pressure leads

to the decline of exergy destruction and exergy loss rates, while the increase in boiler temperature has the opposite effect.

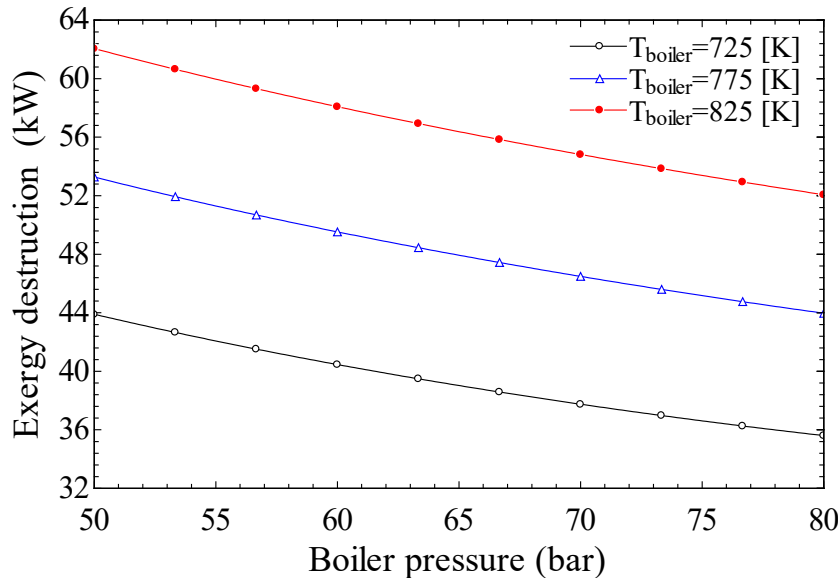


Fig. 12. Exergy destruction rate in the steam cycle versus boiler pressure for different boiler temperatures.

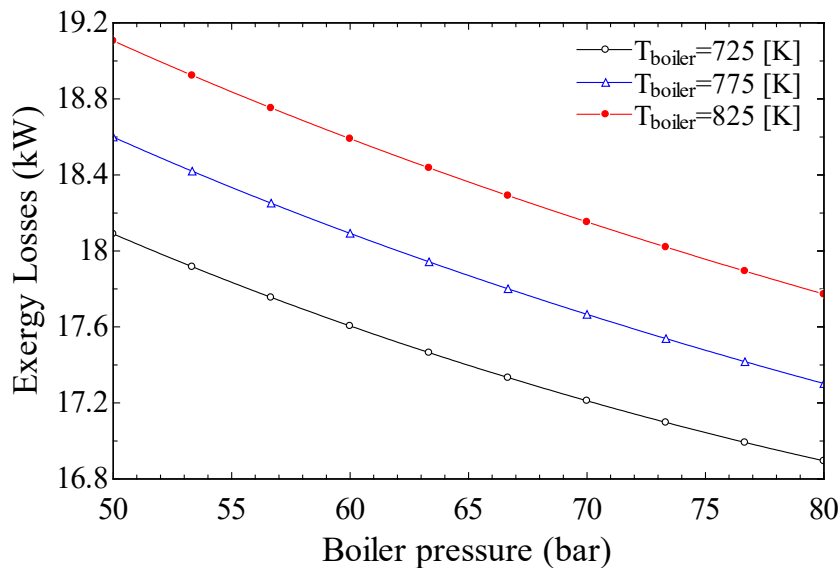


Fig. 13. Rate of exergy loss in the steam cycle versus boiler pressure for different boiler temperatures.

**5.3. Analyzing the results of the GT+SOFC+St hybrid system**

In this section, the results related to the analysis of the triple combined system shown in Fig. 3 are presented and discussed. According to these results, after adding the steam cycle to the dual system of GT-FC, the new hybrid system's (GT+SOFC+St) net power generation increases by 51% in comparison with the simple GT cycle and about 14% in comparison with the GT+SOFC hybrid system. The electrical efficiency of the proposed triple system rises by about 52% in comparison with the simple GT cycle and about 13% in comparison with the GT+SOFC hybrid system. This cycle was also placed in the path of gas turbine

outlet gases to investigate the effect of changing the steam cycle location. The schematic of this configuration is depicted in Fig. 14. The results illustrated in Fig. 15 show that this change in steam cycle location diminishes the proposed system's output power. The reason for this is the drop in the temperature of the gases used to preheat the fuel and air entering the GT-SOFC hybrid cycle. This drop lowered the fuel cell temperature and reduced its output power. In the second configuration shown in the figure, the outlet gases from the GT directly enter the steam generator; and this increases the output power of the boiler. While as was mentioned above, the amount of power generated by the FC diminishes. The results show that the output power of the GT is almost the same in both configurations.

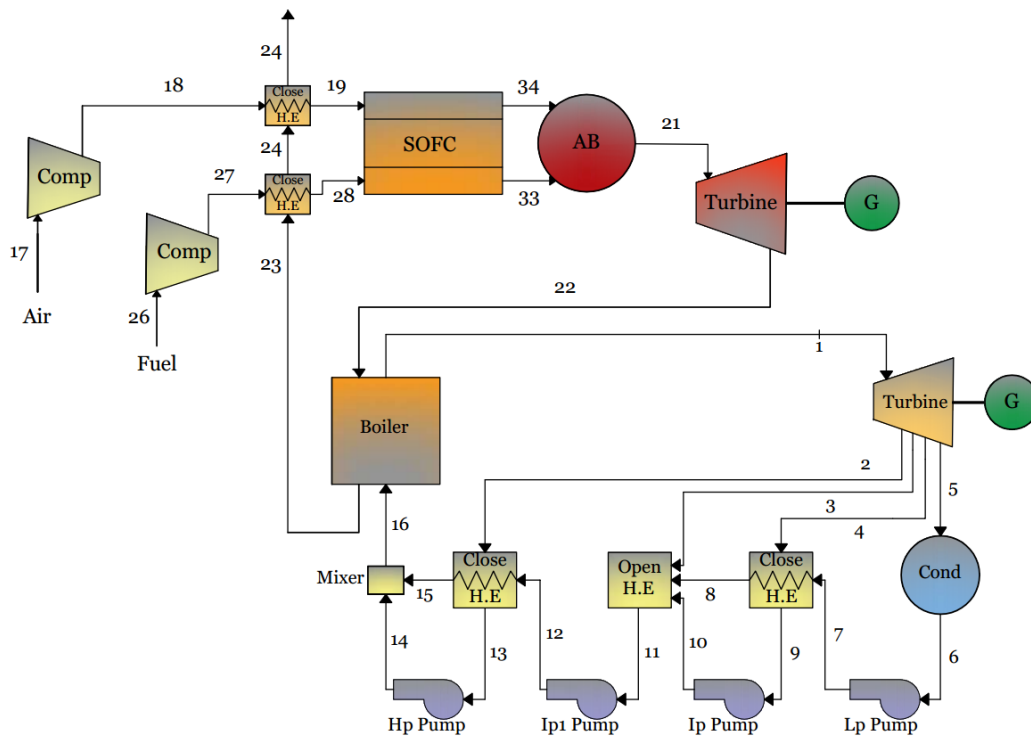


Fig. 14. Placing the steam cycle in the path of gas turbine outlet gases.

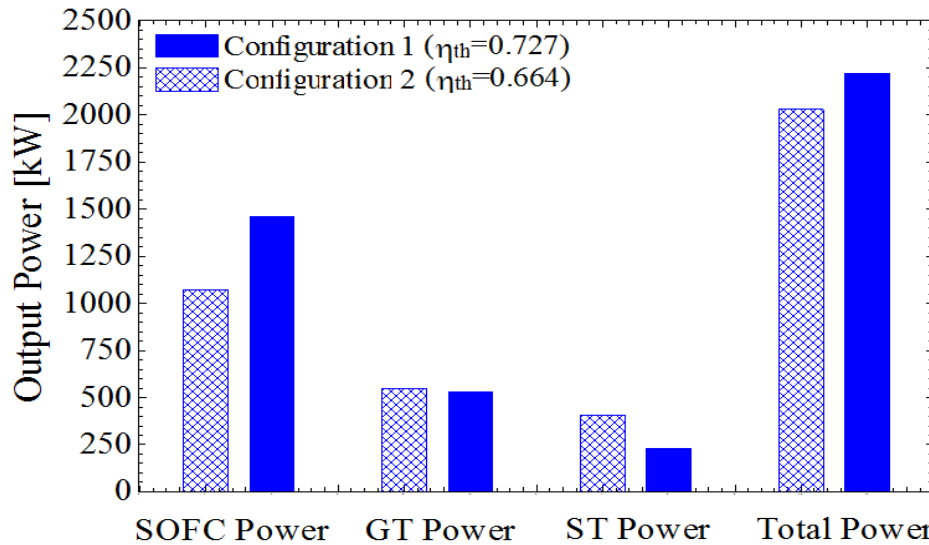


Fig. 15. Comparing the output powers of the triple hybrid system components in two different configurations.

#### 5.4. Analyzing the results of the organic Rankin cycle

In this research, we have also analyzed the performance of the triple combined system by considering an ORC. The schematic of this cycle is presented in Fig. 16. In this section, the effects of five different working fluids on the performance of the ORC were evaluated, and the most suitable working fluid was selected for use in the proposed triple hybrid system.

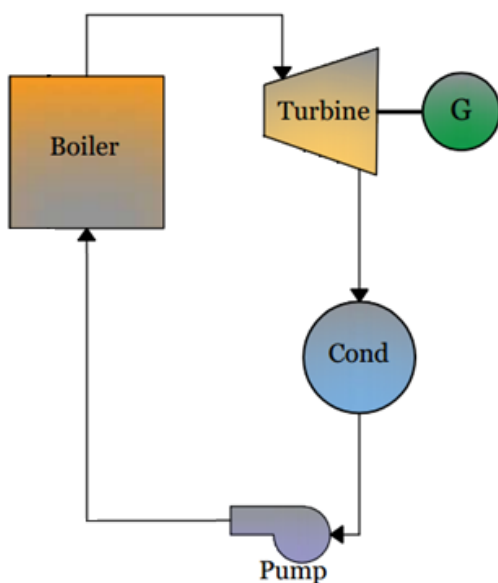


Fig. 16. Schematic of the organic Rankin cycle.

The saturated vapor temperature of the working fluid used in the organic Rankin cycle is considerably less than that of the steam cycle; also, the process flow-chart of this cycle differs from that of the steam cycle. These differences create a large discrepancy in the behaviors and operations of the two cycles. For analyzing the organic Rankin cycle, two cases were considered. In the first case, the condenser temperature is lower than the ambient temperature, and in the second case, it is higher. In the first case, a condenser pressure of 0.1 bar has been considered. In this case, for some fluids, the condenser temperature appropriate for such pressure is lower than the ambient temperature; and naturally, heat does not dissipate to the environment under these conditions. Therefore, a cold source should be considered to use these working fluids in ambient conditions, which does not seem rational. In order to deal with this problem, in the second case, the condenser temperature was assumed to be higher than the ambient temperature so that heat could be discharged to the surrounding environment. In the second case, the condenser pressure consistent with this temperature is also computed. Figs. 17 and 18, related to the first case, illustrate the output powers and the electrical efficiencies of the organic Rankin cycle for

condenser pressure of  $P_{\text{cond}} = 0.1$  bar, respectively. As is observed, under the stated conditions, the R123 organic fluid achieves the highest efficiency and output power among the examined working fluids. However, considering the low temperature of the condenser, a low-temperature source would be needed in this case.

working fluid of toluene are substantially greater than those obtained by other fluids. The given condenser temperature, with regards to toluene, is in line with the pressure of 0.1 bar. The results indicate that, at the constraints applied to the cycle, toluene has the best performance among the other working fluids used.

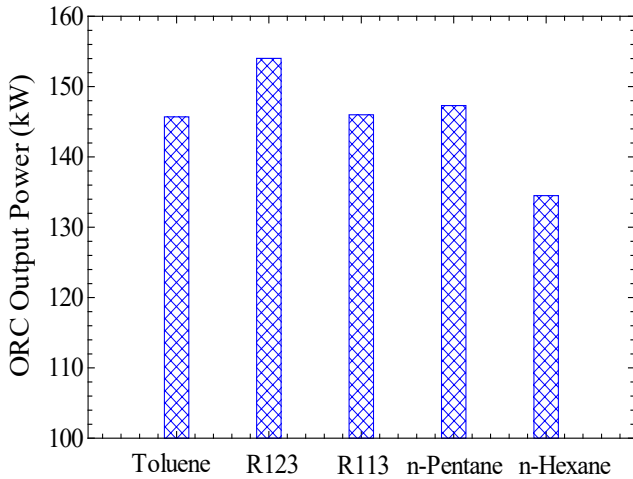


Fig. 17. Comparing the output powers of the organic Rankin cycle for different working fluids ( $P_{\text{cond}} = 0.1$  bar).

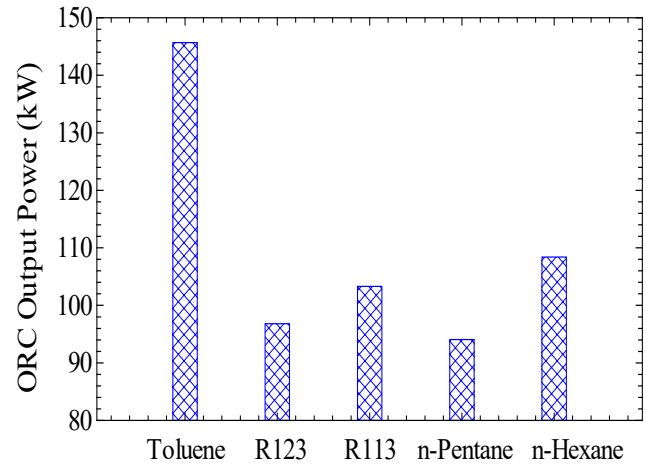


Fig. 19. Comparing the output powers of the organic Rankin cycle for different working fluids ( $T_{\text{cond}} = 319$  K).

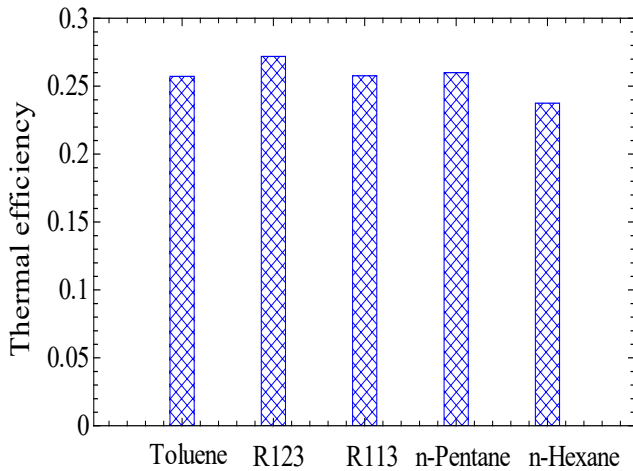


Fig. 18. Comparing the electrical efficiencies of the organic Rankin cycle for different working fluids ( $P_{\text{cond}} = 0.1$  bar).

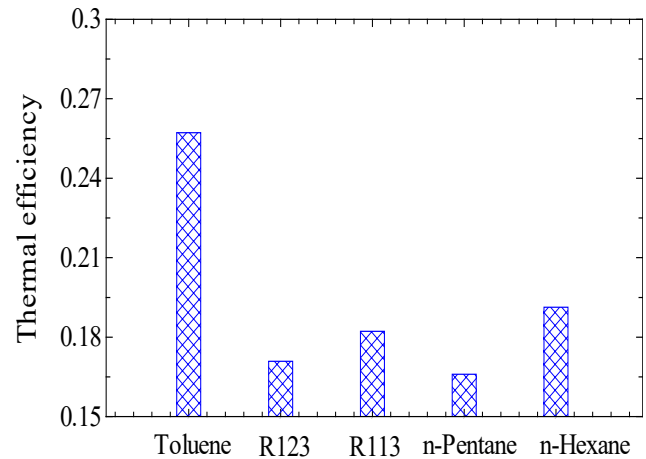


Fig. 20. Comparing the electrical efficiencies of the organic Rankin cycle for different working fluids ( $T_{\text{cond}} = 319$  K).

In Figs. 19 and 20, related to the second case, the output power and the electrical efficiency of the organic Rankin cycle have been plotted for a condenser temperature of  $T_{\text{cond}} = 319$  K. As is seen, the output power and the cycle efficiency achieved by using the

The analyses performed on the organic Rankin cycle revealed that the toluene working fluid is the best organic fluid among the five examined fluids. Next, the organic Rankin cycle with toluene as the working fluid was compared with the simple steam cycle. The

results of this comparison are illustrated in Figs. 21 and 22. In this section, two different cycles have been evaluated for the same input temperature from the upstream cycle. As shown in these two figures, the two examined cycles have different working paths, and, with the given conditions, the output power of the

steam cycle is greater than that of the organic Rankin cycle. The turbine input temperature in the organic Rankin cycle is considerably lower than in the steam cycle, which allows the organic Rankin cycle to be used in low-temperature heat regenerators.

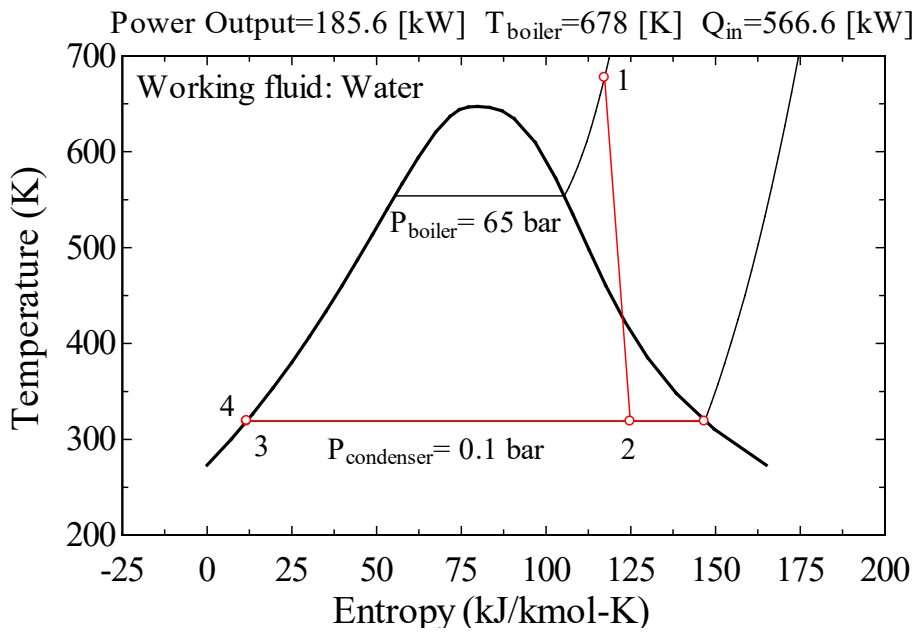


Fig. 21. The temperature-entropy graph for the steam Rankin cycle.

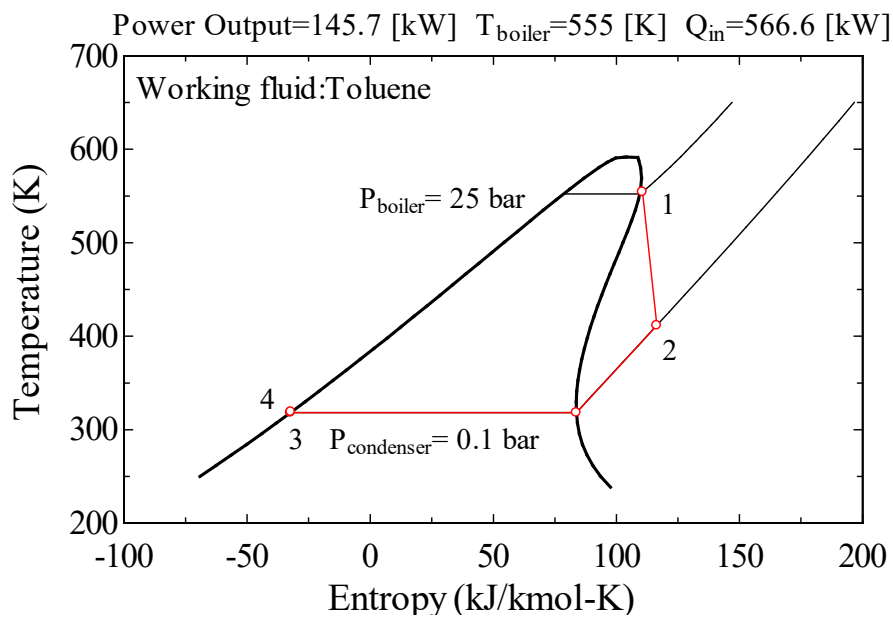


Fig. 22. The temperature-entropy graph for the organic Rankin cycle with toluene as the working fluid.

The T-S graphs for water vapor and five organic fluids have been plotted in Fig. 23. The operational differences between these fluids can be seen in this figure. Considering the positive slope of the vapor saturation line for toluene, this organic fluid does not become

two-phase during the expansion process in the turbine. However, it changes to superheated steam at lower pressures. Therefore, it is not necessary to superheat the turbine input steam when using toluene.

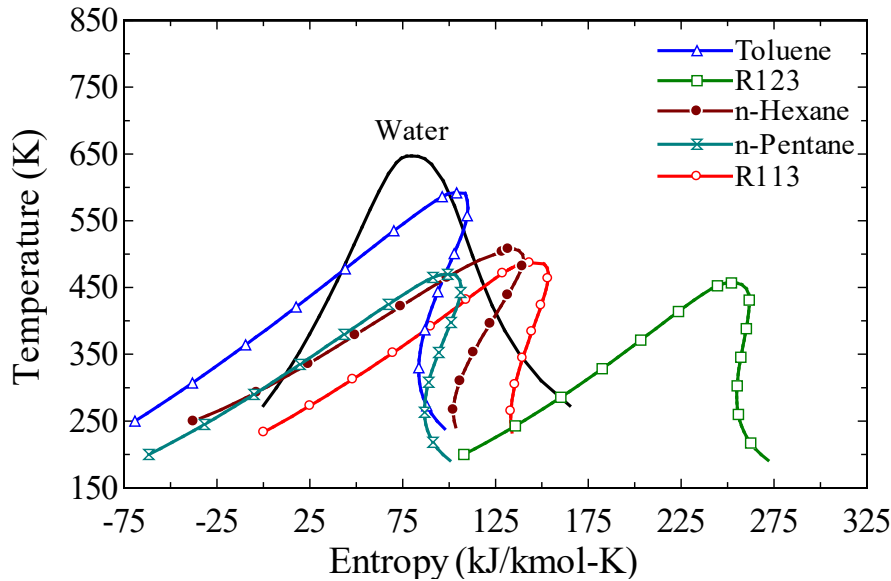


Fig. 23. Comparing the effects of using different working fluids in the ORC.

### 5.5 . Analyzing the results of the triple combined system with the organic Rankin cycle

A schematic of the triple integrated system with the organic Rankin cycle is presented in Fig. 24. Based on the obtained results, adding the steam cycle and the organic Rankin cycle to the dual hybrid system of GT+SOFC increases the electrical efficiency and the net generated power of the resulting triple integrated system. Fig. 25 shows the output powers of the triple combined system for two cases: a steam cycle and an organic Rankin cycle. According to this figure, the output power of the combined cycle plus the steam cycle is greater than that of the hybrid system with the organic Rankin cycle; however, this higher power

output does not necessarily mean that this cycle is better. In a microturbine cycle, with regards to the limited inlet gases temperature of the turbine (maximum temperature of 1000 °C), the discharged gases from this system have a low temperature, and normally, it is not possible to start up a steam cycle (with the minimum superheated vapor temperature of about 400 °C) in this case. However, considering the lower saturated vapor temperature in the organic Rankin cycle (about 280 °C), this cycle can be implemented. Therefore, the use of a steam cycle in the hybrid system will be more justified by greater power outputs and higher temperatures of turbine inlet gases because the outlet gases from the gas turbine cycle will have a higher temperature.

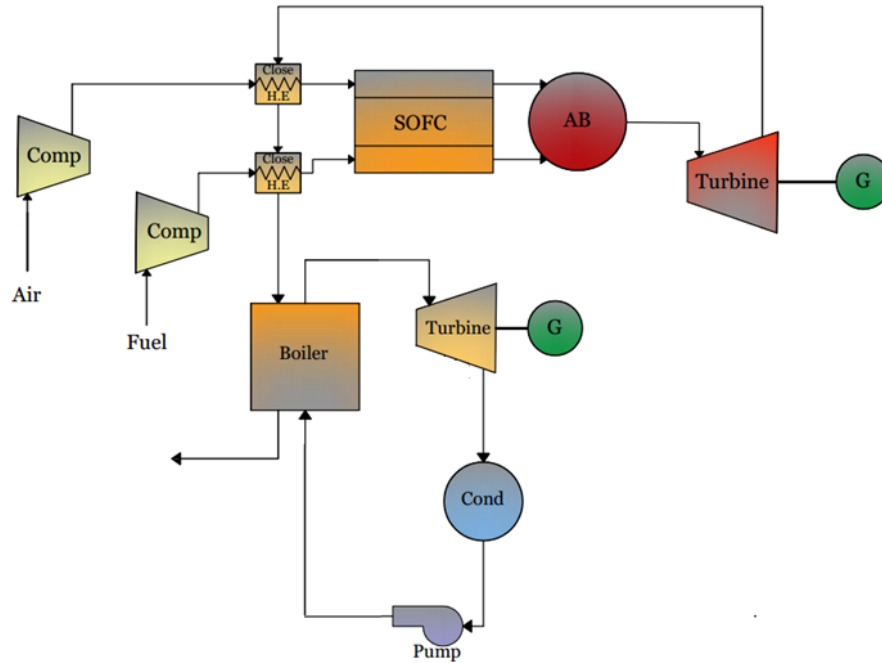


Fig. 24. Schematic of the integrated system of GT, fuel cell, and organic Rankin cycle.

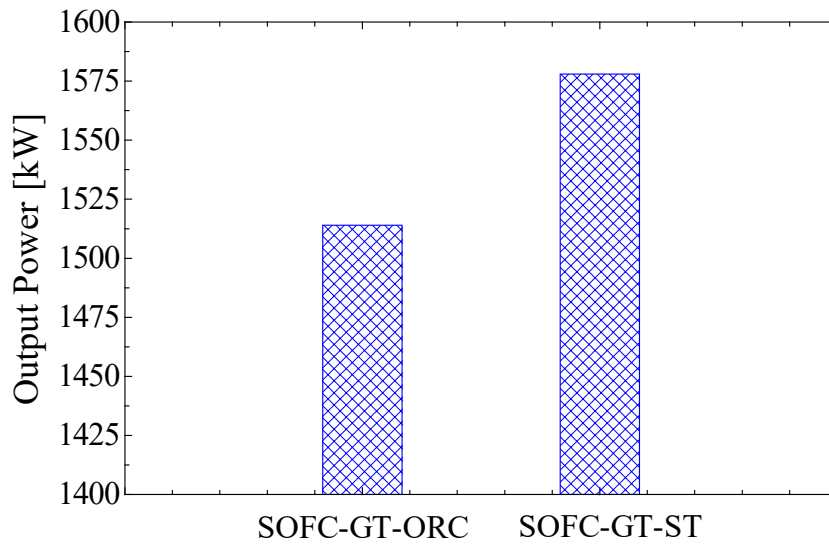


Fig. 25. Comparing the output powers of two types of triple hybrid systems.

## 6- Conclusion

In this section, the important findings of this research are summarized and presented:

- The net power generation of the proposed hybrid system (GT+SOFC+St) increases by 51% compared

to the simple GT cycle and about 14% compared to the GT+SOFC hybrid system. The electrical efficiency of the proposed triple combined system increases by 52% compared to the simple GT cycle and about 13% compared to the GT+SOFC hybrid system.

- By changing the location of the steam cycle and

placing it at the beginning section of the path of discharged gases from the GT+SOFC integrated system, the net output power of the triple combined system diminishes. The results show that preheating the inlet fuel and air of the GT+SOFC cycle has a better effect on the system's performance, and it is better to place the steam cycle after the air and fuel regenerators of this cycle.

- At the condenser temperature of 319 °K, the proposed triple hybrid system produces the largest amount of output power by using toluene in the organic Rankin cycle (as compared to the other considered organic fluids).
- The output power of the combined cycle plus the steam cycle is greater than the hybrid system with the organic Rankin cycle; however, this higher power output does not necessarily mean that this cycle is better. The use of a steam cycle in the hybrid system will be more justified by greater power outputs and higher temperatures of turbine inlet gases.

## References

- [1]He, Ting, and Wensheng Lin. "Energy saving research of natural gas liquefaction plant based on waste heat utilization of gas turbine exhaust." *Energy Conversion and Management* 225 (2020): 113468.
- [2]Musharavati, Farayi, Shoaib Khanmohammadi, Amirhossein Pakseresht, and Saber Khanmohammadi. "Waste heat recovery in an intercooled gas turbine system: Exergo-economic analysis, triple objective optimization, and optimum state selection." *Journal of Cleaner Production* 279 (2021): 123428.
- [3]Pirkandi, Jamasb, Arman Maroufi, and Shahram Khodaparast. "Parametric simulation and performance analysis of a solar gas turbine power plant from thermodynamic and exergy perspectives." *Journal of Mechanical Science and Technology* 32, no. 5 (2018): 2365-2375.
- [4]Maheshwari, Mayank, and Onkar Singh. "Comparative evaluation of different combined cycle configurations having simple gas turbine, steam turbine and ammonia water turbine." *Energy* 168 (2019): 1217-1236.
- [5]Maroufi, Arman, Jamasb Pirkandi, and Mohammad Ommian. 2022. "Exergy and Economic Investigation of Different Strategies of Hybrid Systems Consisting of Gas Turbine (GT) and Solid Oxide Fuel Cell (SOFC)". *International Journal of Integrated Engineering* 14 (1):127-39.
- [6]Carapellucci, Roberto, and Lorena Giordano. "Regenerative gas turbines and steam injection for repowering combined cycle power plants: Design and part-load performance." *Energy Conversion and Management* 227 (2021): 113519.
- [7]He, Yijian, Shupeng Zheng, and Gang Xiao. "Solar hybrid steam-injected gas turbine system with novel heat and water recovery." *Journal of Cleaner Production* 276 (2020): 124268.
- [8]Hosseini, Seyed Ehsan. "Design and analysis of renewable hydrogen production from biogas by integrating a gas turbine system and a solid oxide steam electrolyzer." *Energy Conversion and Management* 211 (2020): 112760.
- [9]Rossi, Iacopo, Alberto Traverso, and David Tucker.

- “SOFC/Gas Turbine Hybrid System: A simplified framework for dynamic simulation.” *Applied Energy* 238 (2019): 1543-1550.
- [10] Jamasb Pirkandi, Majid Ghassemi, Mohammad Hossein Hamedi. “Performance comparison of direct and indirect hybrid systems of gas turbine and solar oxide fuel cell from thermodynamic and exergy viewpoints”, *Modares Mechanical Engineering*, Volume:12 Issue:3 (2012): 117-133.
- [11] Pirkandi, J., and Ommian, M. (May 9, 2018). “Thermo-Economic Operation Analysis of SOFC–GT Combined Hybrid System for Application in Power Generation Systems.” ASME. *J. Electrochem. En. Conv. Stor.* February 2019; 16(1): 011001.
- [12] Lai, Haoxiang, Nor Farida Harun, David Tucker, and Thomas A. Adams II. “Design and eco-technoeconomic analyses of SOFC/GT hybrid systems accounting for long-term degradation effects.” *International Journal of Hydrogen Energy* 46, no. 7 (2021): 5612-5629.
- [13] Pirkandi, J., Jahromi, M., Sajadi, S.Z. *et al.* Thermodynamic performance analysis of three solid oxide fuel cell and gas microturbine hybrid systems for application in auxiliary power units. *Clean Techn Environ Policy* **20**, 1047–1060 (2018).
- [14] Lai, Haoxiang, Nor Farida Harun, David Tucker, and Thomas A. Adams II. “Design and Eco-technoeconomic Analyses of SOFC/Gas Turbine Hybrid Systems Accounting for Long-Term Degradation.” In *Computer Aided Chemical Engineering*, vol. 48, pp. 415-420. Elsevier, 2020.
- [15] Eisavi, Beneta, Ata Chitsaz, Javad Hosseinpour, and Faramarz Ranjbar. “Thermo-environmental and economic comparison of three different arrangements of solid oxide fuel cell-gas turbine (SOFC-GT) hybrid systems.” *Energy Conversion and Management* 168 (2018): 343-356.
- [16] Huang, Yu, and Ali Turan. “Mechanical equilibrium operation integrated modelling of recuperative solid oxide fuel cell–gas turbine hybrid systems: Design conditions and off-design analysis.” *Applied Energy* (2020): 116237.
- [17] Hedberg, Garrett, Ryan Hamilton, and Dustin McLarty. “Design and performance analysis of a de-coupled solid oxide fuel cell gas turbine hybrid.” *International Journal of Hydrogen Energy* 45, no. 55 (2020): 30980-30993.
- [18] Guo, Yinglun, Zeting Yu, Guoxiang Li, and Hongxia Zhao. “Performance assessment and optimization of an integrated solid oxide fuel cell-gas turbine cogeneration system.” *International Journal of Hydrogen Energy* 45, no. 35 (2020): 17702-17716.
- [19] Azizi, Mohammad Ali, and Jacob Brouwer. “Progress in solid oxide fuel cell-gas turbine hybrid power systems: System design and analysis, transient operation, controls and optimization.” *Applied energy* 215 (2018): 237-289.
- [20] Pirkandi, Jamasb, Hossein Penhani, and Arman Maroufi. “Thermodynamic analysis of the performance of a hybrid system consisting of steam turbine, gas turbine and solid oxide fuel cell (SOFC-GT-St).” *Energy Conversion and Management* 213 (2020): 112816.
- [21] Ezzat, M. F., and I. Dincer. “Energy and exergy analyses of a novel ammonia combined power

- plant operating with gas turbine and solid oxide fuel cell systems.” *Energy* 194 (2020): 116750.
- [22]Chen, Yunru, Meng Wang, Vincenzo Liso, Sheila Samsatli, Nouri J. Samsatli, Rui Jing, Jincan Chen, Ning Li, and Yingru Zhao. “Parametric analysis and optimization for exergoeconomic performance of a combined system based on solid oxide fuel cell-gas turbine and supercritical carbon dioxide Brayton cycle.” *Energy Conversion and Management* 186 (2019): 66-81.
- [23]Al-Hamed, K. H. M., and I. Dincer. “A new direct ammonia solid oxide fuel cell and gas turbine based integrated system for electric rail transportation.” *ETransportation* 2 (2019): 100027.
- [24]Minutillo, Mariagiovanna, Alessandra Perna, Elio Jannelli, Viviana Cigolotti, Suk Woo Nam, Sung Pil Yoon, and Byeong Wan Kwon. “Coupling of biomass gasification and SOFC–gas turbine hybrid system for small scale cogeneration applications.” *Energy procedia* 105 (2017): 730-737.
- [25]Yuksel, Yunus Emre, Murat Ozturk, and Ibrahim Dincer. “Performance investigation of a combined biomass gasifier-SOFC plant for compressed hydrogen production.” *International Journal of Hydrogen Energy* 45, no. 60 (2020): 34679-34694.
- [26]Gholamian, E., and V. Zare. “A comparative thermodynamic investigation with environmental analysis of SOFC waste heat to power conversion employing Kalina and Organic Rankine Cycles.” *Energy Conversion and Management* 117 (2016): 150-161.
- [27]Kim, Young Sang, Young Duk Lee, and Kook Young Ahn. “System integration and proof-of-concept test results of SOFC–engine hybrid power generation system.” *Applied Energy* 277 (2020): 115542.
- [28]Sadat, Seyed Mohammad Sattari, Hadi Ghaebi, and Arash Mirabdollah Lavasani. “4E analyses of an innovative polygeneration system based on SOFC.” *Renewable Energy* 156 (2020): 986-1007.
- [29]Mehrpooya, Mehdi, Bahram Ghorbani, and Hadi Abedi. “Biodiesel production integrated with glycerol steam reforming process, solid oxide fuel cell (SOFC) power plant.” *Energy Conversion and Management* 206 (2020): 112467.
- [30]Chan, S. H., H. K. Ho, and Y. Tian. “Modelling of simple hybrid solid oxide fuel cell and gas turbine power plant.” *Journal of power sources* 109, no. 1 (2002): 111-120.
- [31]Cengel, Yunus A., and Michael A. Boles. *Thermodynamics: An Engineering Approach 6th Edition (SI Units)*. The McGraw-Hill Companies, Inc., New York, 2007.
- [32]Song, Jian, Chun-wei Gu, and Xiaodong Ren. “Parametric design and off-design analysis of organic Rankine cycle (ORC) system.” *Energy Conversion and Management* 112 (2016): 157-165.